Performance of the Blending Factor Approach for Modeling the Interfacial Forces in Bubble Columns Operating at High Gas Hold Up

14th International Conference on CFD in Oil & Gas, Metallurgical and Process Industries
SINTEF, Trondheim, NORWAY
October 12-14, 2020

PERFORMANCE OF THE BLENDING FACTORS APPROACH FOR MODELING THE INTERFACIAL FORCES IN BUBBLE COLUMNS OPERATING AT HIGH GAS HOLD UP

Francesco MANISCALCO[1*], **Mohsen SHIEA**[1], **Antonio BUFFO**[1], **Daniele MARCHISIO**[1], **Marco VANNI**[1†]

[1]Department of Applied Science and Technology, Politecnico di Torino, ITALY

[*] E-mail: francesco.maniscalco@polito.it
[†] E-mail: marco.vanni@polito.it

ABSTRACT

Gas-liquid bubble columns are commonly used in the process industry due to their ease in construction and their excellent performances. However, the formulation of numerical models of such industrial-scale systems is troublesome especially because of the strong coupling between the phases. In fact, it is crucial to properly describe the phase coupling in the Euler-Euler framework in terms of the drag and other interfacial forces. This is particularly important at high gas superficial velocity, when the global gas fraction is higher and the drag coefficient is very different from that for isolated particles. One way of addressing the problem is coupling a correction for the swarm effect occurring at relatively high gas fractions with a blending approach, which sets a natural transition of the drag force in the phase inversion region.

The numerical simulations were carried out with the CFD code OpenFOAM. While in commercial codes the application of methods of this kind is not always mentioned, in open-source codes, such as OpenFOAM, it is possible to prescribe completely all the settings of the procedure. As a first step of the work, we performed an accurate study on a proper selection of the blending parameters in order to evaluate the impact on the results. Then, a comparison of the proposed model with experimental data and with simulations available in the literature is performed, showing that blending produces accurate results and significantly increases computational speed, since in both homogeneous and heterogeneous regimes the required computational time has been halved.

Particularly interesting is the comparison between simulations carried out in absence and in presence of blending: in the former case the swarm formulation needs an ad hoc correction to capture correctly the gas hold up. It also shows numerical instability due to the phase inversion occurring at the boundary between liquid and head space of the column. Therefore the blending implementation, with a valid selection of parameters, is preferable since it improves the computational speed and numerical robustness.

Keywords: CFD, hydrodynamics, bubble columns, OpenFOAM, multiphase system .

NOMENCLATURE

Greek Symbols

α	Volume fraction, $[-]$.
ε	Turbulent dissipation rate, $[m^2/s^3]$.
ρ	Mass density, $[kg/m^3]$.
μ	Viscosity, $[kg/ms]$.
μ_T	Turbulent viscosity, $[kg/ms]$.
$\mathbf{\Sigma}$	Stress tensor, $[Pa]$.
σ	Interfacial tension, $[N/m]$.

Latin Symbols

C_D	Drag coefficient, $[-]$.
D	Column diameter, $[m]$.
d_b	Bubble diameter, $[m]$.
$\mathbf{g}$	Gravitational acceleration, $[m/s^2]$.
H	Column height, $[m]$.
h	Swarm factor ,$[-]$.
I	Turbulence intensity, $[-]$.
k	Turbulent kinetic energy, $[m^2/s^2]$.
p	Pressure, $[Pa]$.
R	Column radius, $[m]$.
S	Section area, $[m^2]$.
r	radial coordinate, $[m]$.
$\mathbf{u}$	Velocity, $[m/s]$.
$\langle U \rangle$	Superficial gas velocity, $[m/s]$.
z	axial coordinate. $[m]$.

Sub/superscripts

FD	Fully Dispersed.
G	Gas.
in	Inlet.
k	Phase index k.
L	Liquid.
l	Phase index l.
PD	Partially Dispersed.

INTRODUCTION

Bubble column reactors are nowadays fundamental in industrial equipment: the easiness in construction and the excellent performances in heat and mass transfer have provided them a wide diffusion in chemical, petrochemical and biochemical engineering (Ranade, 2002), ranging from Fischer-Tropsch synthesis (Basha *et al.*, 2015) to microbial digestion (Kantarci *et al.*, 2005).

In the most common configuration the gas phase is injected from the bottom of the column through a sparger and rises through the liquid phase, which may often contain solid catalytic particles (slurry bubble column). The gas is thus dispersed into small bubbles through the liquid, therefore the former may be considered as dispersed phase and the latter as continuous. As a consequence of the injection of the gas, the liquid height rises to a new value corresponding to the sum of the liquid and air volumes: this variation corresponds to the global gas hold-up, which is a key feature in the analysis of the column performances.

In particular, low values of hold-up are peculiar of the so-called homogeneous regime, where the bubbles have approximately the same size and the liquid recirculation is moderate. As the gas superficial velocity, namely the velocity the gas would have if it occupied the whole cross-sectional area, increases, the hold-up increases linearly as well and, after a transition area, starts rising again with a lower slope, hitting hence the heterogeneous regime: the bubbles present a broad variation in size and the liquid recirculation patterns become relevant.

Despite its apparent simplicity, the hydrodynamics of such systems is complicated due to the many types of interaction between dispersed and continuous phase which have a relevant impact on the global behavior. These issues worsen in the heterogeneous regime, which is preferred in industrial applications to maximize the mixing: the larger values of gas fraction and the strong dependency on the radial coordinate of the most notable variables (local hold-up, axial velocity, turbulent quantities) (Shu *et al.*, 2019) have caused non-trivial difficulties when a reliable modeling is desired.

To address this crucial matter, recent research has focused on the expression of the major interfacial forces (Tabib *et al.*, 2008). The most relevant is undoubtedly the drag force, which is due to velocity difference between phases. As the heterogeneous regime is approached, the bubbles get closer and the local gas fraction dramatically increases, eventually leading to a wrong prediction of the drag force and, therefore, of the global hydrodynamics. With the aim to solve this issue, some authors proposed a correction of the drag formula considering the impact of bubbles proximity (swarm effect) (Simonnet *et al.*, 2008; Roghair *et al.*, 2011; McClure *et al.*, 2017). The main drawback of these corrections is either their limited operative range (limited to $\alpha_G \leq 0.1$) or, if formulated for heterogeneous regime, the fact that the predicted correction factor approaches to zero as the hold-up is increased, thus canceling out the whole drag force and giving rise to large regions of high gas volume fraction in the dispersion that are not physical.

This point may be addressed by limiting the swarm correction term to avoid the cancellation of the drag swarm at high gas fraction (Gemello *et al.*, 2018). This correction became necessary because in most of commercial CFD solvers the dispersed and continuity phases must be specified *a priori* throughout the domain: when the gas superficial velocity is high, it may occur that in some portion of the domain the gas fraction is high enough to eliminate the swarm correction although the gas is still the dispersed phase. The swarm correction limitation avoids this type of issues, guaranteeing a non-zero drag term even for large gas fraction values. Unfortunately, in this approach the correction factor must be fitted to match the experimental data of hold up.

On the other hand, the open source software OpenFOAM offers an implementation of the so-called blending parameters, which, through an appropriate selection, allow the solver to distinguish locally the dispersed and the continuous phase. To the best of our knowledge an accurate study of this method has not been attempted in the literature so far: the aim of this study is thus providing an insight of the blending implementation in order to find the best set of parameters for gas-liquid and gas-solid-liquid bubbly flows.

MODEL DESCRIPTION

The gas and liquid phases are both modeled as interpenetrating continuous media according to the Euler-Euler description. In this case, the continuity and Navier-Stokes equations are:

$$\frac{\partial}{\partial t}\alpha_k\rho_k + \nabla\left(\alpha_k\rho_k\mathbf{u}_k\right) = 0 \tag{1}$$

$$\frac{\partial}{\partial t}\alpha_k\rho_k\mathbf{u}_k + \nabla\cdot\left(\alpha_k\rho_k\mathbf{u}_k\mathbf{u}_k\right) = \\ = -\alpha_k\nabla p + \alpha_k\rho_k\mathbf{g} + \nabla\cdot\left(\alpha_k\mathbf{\Sigma}_k\right) + \mathbf{F}_{kl}. \tag{2}$$

The turbulence is implemented as a standard k-ε dispersed model, where only the continuous phase is considered turbulent.

The term $\mathbf{F}_{kl}$ denotes the summation of all the interphase forces occurring between generic phase k and l. In this study the only term considered is the drag force, and, denoting liquid phase as L and gaseous phase as G, it may be formulated as:

$$\mathbf{F}^{\infty}_{D,LG} = \frac{3}{4}C^{\infty}_{D}\frac{\alpha_G\rho_L}{d_b}\left(\mathbf{u}_L - \mathbf{u}_G\right)\left|\mathbf{u}_L - \mathbf{u}_G\right|. \tag{3}$$

(in the following the subscripts LG are dropped in sake of simplicity). The drag coefficient for isolated bubbles can be evaluated from a wide number of correlations (Naumann and Schiller, 1935; Ishii and Zuber, 1979). In this study the one suggested by Tomiyama was used since it is the most suitable for contaminated bubbly gas-liquid systems (Tomiyama, 1998):

$$C^{\infty}_{D} = \max\left[\min\left(\frac{24}{Re}(1+Re^{0.687}), \frac{72}{Re}\right), \frac{8}{3}\frac{Eo}{Eo+4}\right], \tag{4}$$

being Re and Eo respectively the Reynolds and Eötvös number.

The swarm effect is taken into account multiplying C^{∞}_{D} by a semi-empirical factor h (Simonnet *et al.*, 2008)

$$h = \frac{C_D}{C^{\infty}_{D}} = (1-\alpha_G)\left[(1-\alpha_G)^{25} + \left(4.8\frac{\alpha_G}{1-\alpha_G}\right)^{25}\right]^{-2/25} \tag{5}$$

This correlation is often bounded imposing a minimum value of h, namely h_0 (Gemello *et al.*, 2018):

$$h = \max\left(h_{\text{Simonnet}}, h_0\right) \tag{6}$$

h_0 might range from 0.08 to 0.30 and it should be selected according to the gas superficial velocity and geometry in order to fit the experimental hold up. However, this approach may lead to unrealistic calculations of the liquid velocity and the turbulent quantities when α_k reaches the phase-inversion range and, further on, it generates numerical instability in the head space of the column and at the boundary between liquid and head space. The global outcome is a slow simulation, presenting numerical issues and non-physical results.

A possible approach is the so-called symmetric blending: the drag formula in Eq. (3) is multiplied by the liquid volume fraction α_L in such a way that the drag force approaches to zero in the head space. This solution, despite its straightforwardness, may underestimate the drag force and, consequently, the gas fraction in the two-phase system, where $\alpha_L < 1$.

An improvement of this method is offered by the open-source software OpenFOAM (OpenCFD): in the `twoPhaseEulerFoam` solver, it is possible to specify a blending method, which may be linear or hyperbolic, and some blending parameters. Through the specification of the blending parameters, the solver is capable to detect locally

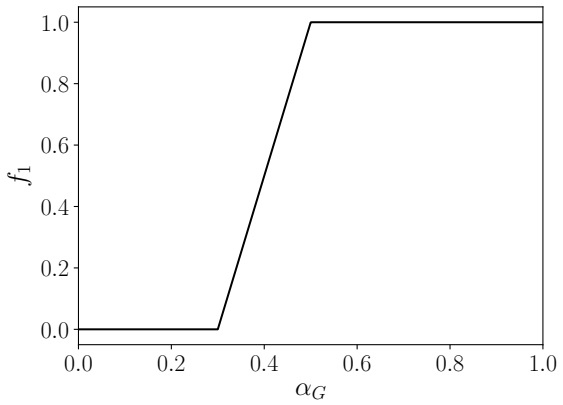

Figure 1: Default linear blending factor f_1.

which phase is dispersed and treat it accordingly. With this aim, two correlations must be specified for every interphase forces coefficient: for phase k dispersed into phase l and vice versa.
In case of linear blending, the code requires 2 parameters per phase:

- `maxFullyDispersedAlpha` (here referred as α_{FD}) defines the gas fraction range $[0, \alpha_{FD}]$ where the phase is modeled as completely dispersed;
- `maxPartialDispersedAlpha` (here referred as α_{PD}), which is the largest value of α_k for the phase to be modeled as dispersed, even if partially.

The blending is achieved by a definition of the blending parameter f for each phase. For the gas phase the blending parameter f_1 is defined as:

$$f_1(\alpha_G) = \min\left[\max\left(\frac{\alpha_G - \alpha_{G,FD}}{\alpha_{G,PD} - \alpha_{G,FD}}, 0\right), 1\right] \quad (7)$$

while, similarly, the blending parameter for the liquid phase is f_2:

$$f_2(\alpha_L) = \min\left[\max\left(\frac{\alpha_{L,PD} - \alpha_L}{\alpha_{L,PD} - \alpha_{L,FD}}, 0\right), 1\right] \quad (8)$$

In the case of $\alpha_{G,FD} = 0.3$ and $\alpha_{G,PD} = 0.5$ (default values in `twoPhaseEulerFoam`) the plot of the blending factor f_1 is provided in Fig. 1.
In the general approach two drag forces and associated blending factors must be computed: bubbles in water (a/w) and drops in air (w/a), respectively. The interphase momentum term is crucial in bubbly flows and in this study it coincides with the drag force. It is blended according to the local air volume fraction through the f_1 factor as it follows:

$$\mathbf{F}_D^{\text{new}} = \mathbf{F}_D^{a/w}(1 - f_1) + \mathbf{F}_D^{w/a}(f_2 - f_1). \quad (9)$$

The formation of aerosol is beyond the scope of this work, a model for the water drop dispersion in air is hence omitted and the second term in the RHS of (9) is dropped.
For each computational node there are three possible scenarios, according to the local value of α_G:

a) $\alpha_G \leq \alpha_{G,FD}$. The air is fully dispersed into water and the whole drag formulation as in Eq. (3) is applied;

b) $\alpha_G > \alpha_{G,PD}$. The air fraction is outside the dispersion range, thus the drag term related to air dispersion in water is null;

c) $\alpha_{G,FD} < \alpha_G \leq \alpha_{G,PD}$. The air is partially dispersed and the drag formula is adjusted according to Eq. (9).

Although the blending was introduced to improve the prediction of the drag force in the two phase region, an additional advantage of the method is the absence of numerical convergence issues in the head space: here, if the blending is not implemented, the solver tries to calculates the drag force for the air-in-water system even if the amount of liquid is completely negligible. That often leads to divergence in the computation of the velocity and turbulence fields. However, through the blending factors specification, in the head space the water switches from being continuous to dispersed and the numerical issues are thus overcome. The final result is a faster and more stable simulation.
It is clear that $\alpha_{k,FD}$ and $\alpha_{k,PD}$ must be chosen wisely in order to obtain physical-sounding results and to maintain the simulations fast and stable. With this aim, a study on a wide range of values was performed and will be discussed in the Results section.

Computational settings

The simulated system in this study is a cylindrical air-water bubble column. The details of the system are provided in Tab. 1 and Tab. 2; the gas density ρ_G is calculated in accordance with the ideal gas law. Experimental data for comparisons are extracted from literature (Raimundo, 2015; Gemello *et al.*, 2018).

Table 1: Properties of the system.

Property	Value	Units
T	25	°C
p	1	bar
μ_L	1.003	mPa s
ρ_L	998.2	kg m^{-3}
μ_G	0.0182	mPa s
σ	0.072	N m^{-1}
d_b	6.5	mm
$\langle U \rangle$	0.03-0.09-0.16	m s^{-1}

Table 2: Geometrical features of the system.

Property	Value	Units
D	0.400	m
H	3.6	m

The domain was discretized in a 45'000 cells mesh depicted in Fig. 2 and Fig. 3: this discretization should guarantee mesh-independent results (Gemello *et al.*, 2018). In particular, at the bottom a thin outer ring was excluded from the inlet section (red area in Fig. 3) to prevent computational issues possible due to gas accumulation at the wall.
Simulations were performed using the `twoPhaseEulerFoam` solver in OpenFOAM 5.0 at various gas superficial velocities in order to investigate both homogeneous and heterogeneous regimes.
The van Leer scheme (van Leer, 1974) was used as discretization scheme for the pressure and velocity equations, while an upwind scheme was used for k and ε. Boundary conditions are summarized in Tab. 3.

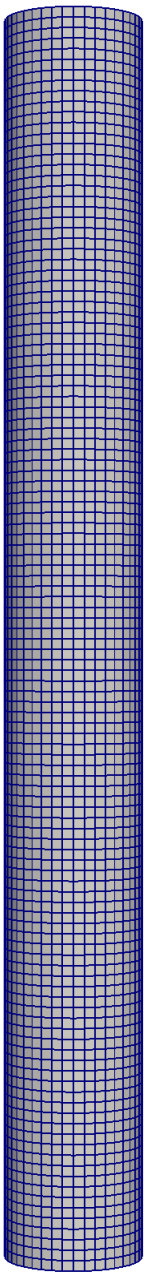

Figure 2: Side view.

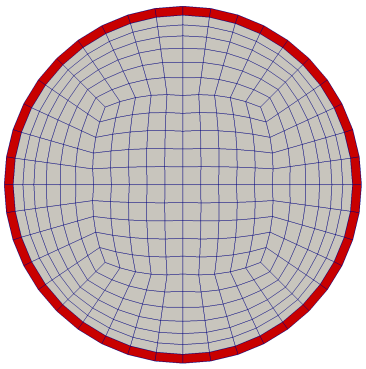

Figure 3: Bottom view. Red area is not included in the sparger.

Transient simulations were performed: each case was simulated for 180 s and it was initialized with the liquid static height equal to 1.6 m and no air dispersion in it. The first order Euler implicit method was used as time-advancement scheme, and an adjustable time step was chosen such in a way that the maximum Courant number was 0.65. The PIMPLE algorithm with 2 inner iterations and a maximum number of 30 outer iterations was adopted for the transient pressure-velocity coupling. The absolute tolerance for every equation was set to $1{\cdot}10^{-7}$.
The results presented in the following sections are obtained through time-averaging the transient data over the last 100 s of simulation.

RESULTS

Impact of input parameters

Firstly a study of the variation impact of $\alpha_{G,FD}$ and $\alpha_{G,PD}$ on the hydrodynamics of the system was performed (in the following the two parameters will always refer to the gas phase: for sake of simplicity, the G subscript will be dropped). This set of simulations was executed for a superficial gas velocity $\langle U \rangle = 0.16$ m s^{-1}: the heterogeneous regime is indeed more complex to simulate and, once the optimal set of parameters is found, they can be easily applied to lower superficial velocity. However, in order to perform a sensitivity study on α_{FD}, it is necessary to set α_{PD} a reasonable value which will we be verified *a posteriori*. In the literature it may be found that for air-in-water dispersion the gas fraction corresponding to the maximum close-packing state of bubbles is approximately 0.75 (Hibiki and Ishii, 2000). Therefore, α_{PD} was set to 0.8 as first value.
Fig. 4 and Fig. 5 present the air fraction and liquid axial velocity profiles for α_{FD} ranging from 0.2 to 0.5 and compare them with experimental data. The effect of the blending factor variation is very small in the prediction of the velocity field, while it becomes more relevant when dealing with the calculation of the air distribution in water. In particular, the wider discrepancies occur in the center of the column where the gas fraction is higher and falls into the $[\alpha_{FD}, \alpha_{PD}]$ interval, with the lowest profile corresponding to α_{FD} equal to 0.2.The increase of this latter parameter causes a shift of the partial dispersion area to higher volume fraction, with a consequent spread of the fully dispersion area. The final outcome is that multiplicative factor $(1 - f_1)$ in Eq. (9) boosts up enlarging α_{FD}, eventually leading to a heavier evaluation of the drag force and, as a final consequence, to a higher local gas fraction. The most effective value for α_{FD} thus seems 0.2, since it both broadens out the partial dispersion region and it provides results closer to experimental data.

Table 3: Boundary conditions.

Var.	Inlet	Outlet	Walls
α_G	0.5	1 for backflow	`zeroGradient`
$\mathbf{u}_G$	$\frac{\langle U \rangle S}{\alpha_{(G,\text{in})} S_{\text{in}}}$	`pressureInletOutletVelocity`	`slip`
$\mathbf{u}_L$	0	`pressureInletOutletVelocity`	`noSlip`
k	$I = 0.05$	$I = 0.001$	`kqRWallFunction`
ε	$\mu_T/\mu = 10$	length scale = $0.7D$	`epsilonWallFunction`

Secondly, after setting α_{FD} to 0.2, the simulations were repeated using 0.7 and 0.8 for α_{PD} to investigate its actual relevance in hydrodynamics of the system: results are shown in Fig. 6 and Fig. 7. The two values provide indistinguishable outcomes, therefore the choice fell on 0.8 since it provides a softer transition between fully dispersion and inversion zones (slope of f_1 in Fig. 1).

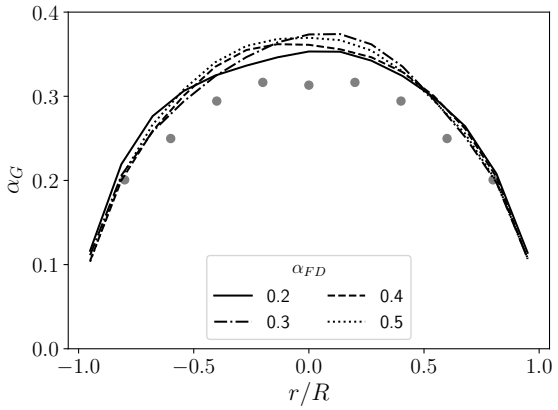

Figure 4: Impact of α_{FD} on gas fraction profiles at height $z/D = 2.5$ and $\langle U \rangle = 0.16\,\mathrm{m\,s^{-1}}$: comparison with experimental data (circles).

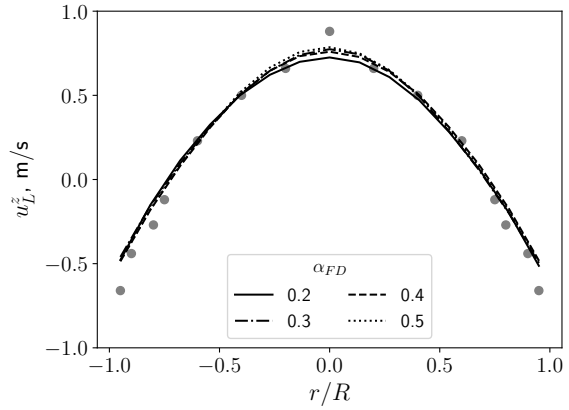

Figure 5: Impact of α_{FD} on liquid z-velocity profiles at height $z/D = 3.75$ and $\langle U \rangle = 0.16\,\mathrm{m\,s^{-1}}$: comparison with experimental data (circles).

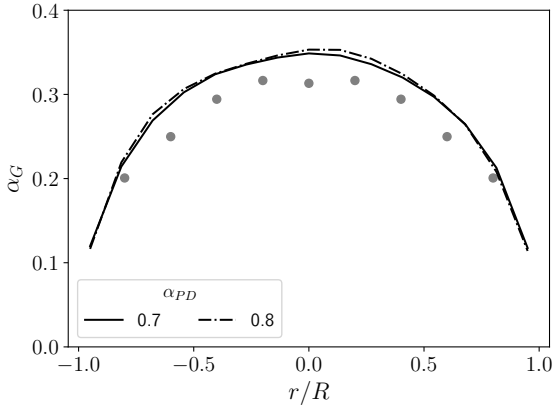

Figure 6: Impact of α_{PD} on gas fraction profiles at height $z/D = 2.5$ and $\langle U \rangle = 0.16\,\mathrm{m\,s^{-1}}$: comparison with experimental data (circles).

In any case, the simulations are not particularly sensitive to the values of α_{FD} or α_{PD}, provided that they are chosen in a reasonable range. From this point of view, the predictions of the blending approach appear quite robust.

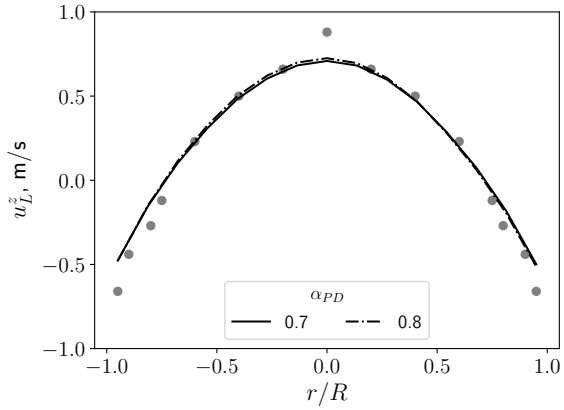

Figure 7: Impact of α_{PD} on liquid z-velocity profiles at height $z/D = 3.75$ and $\langle U \rangle = 0.16\,\mathrm{m\,s^{-1}}$: comparison with experimental data (circles).

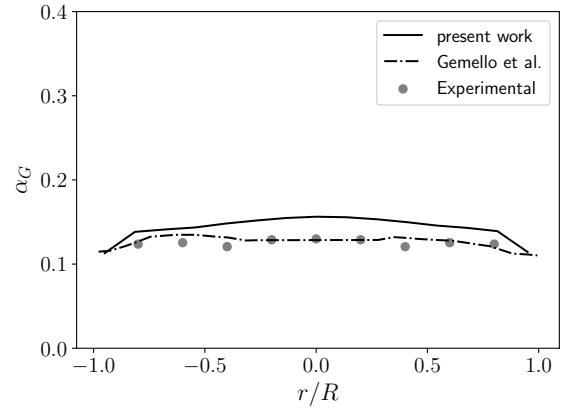

Figure 8: Gas fraction profiles at height $z/D = 2.5$ at $\langle U \rangle = 0.03\,\mathrm{m\,s^{-1}}$ (homogeneous regime): comparison with (Gemello *et al.*, 2018) and experiments.

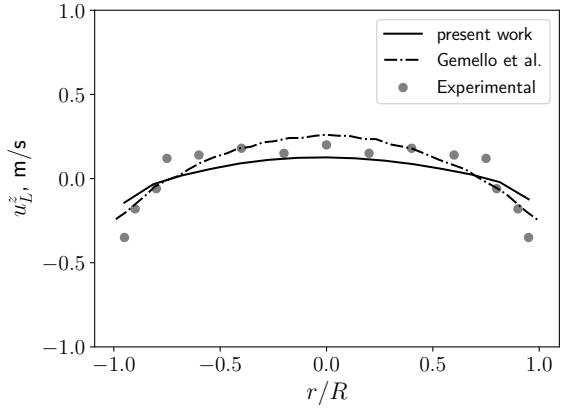

Figure 9: Liquid z-velocity profiles at height $z/D = 3.75$ at $\langle U \rangle = 0.03\,\mathrm{m\,s^{-1}}$ (homogeneous regime): comparison with (Gemello *et al.*, 2018) and experiments.

Results accuracy

The results above-mentioned were then compared to the results obtained by other CFD simulations of the same system (Gemello *et al.*, 2018) executed without the blending factor, but fixing a minimum value of the swarm factor. Computational and modeling settings were set as much as possible identical to the compared work, with the sole exception of turbulence. In accordance with the recent literature, reporting that the RNG k-ε model may provide more realistic results (Syed *et al.*, 2018; Fleck and Rzehak, 2019) for the volume fraction prediction, Gemello et al. modeled the turbulence correspondingly. However, in `twoPhaseEulerFoam` is

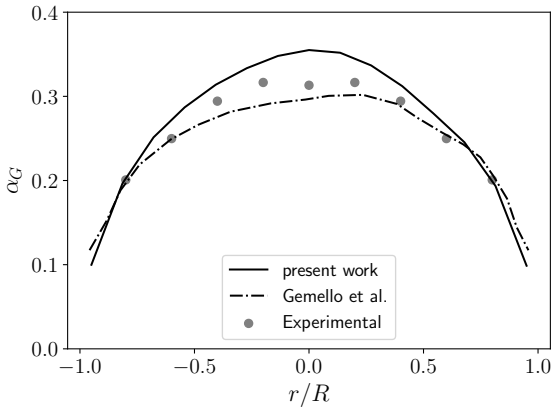

Figure 10: Gas fraction profiles at height $z/D = 2.5$ at $\langle U \rangle = 0.16$ m s^{-1} (heterogeneous regime): comparison with (Gemello *et al.*, 2018) and experiments.

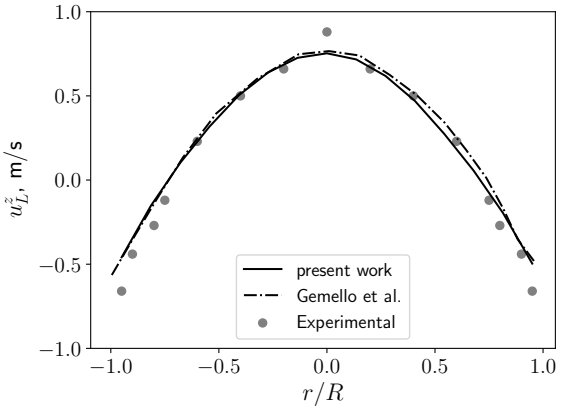

Figure 11: Liquid z-velocity profiles at height $z/D = 3.75$ at $\langle U \rangle = 0.16$ m s^{-1} (heterogeneous regime): comparison with (Gemello *et al.*, 2018) and experiments.

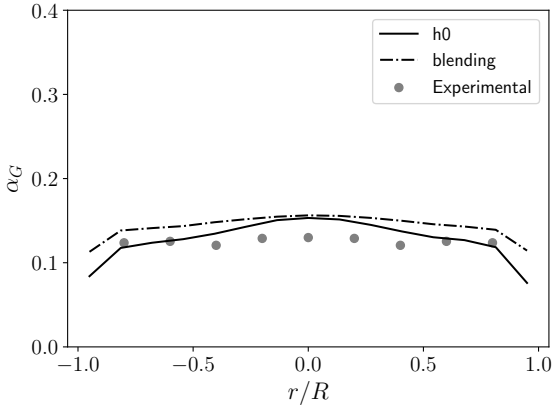

Figure 12: Gas fraction profiles at height $z/D = 2.5$ at $\langle U \rangle = 0.03$ m s^{-1} (homogeneous regime): comparison between the usage of $h_0 = 0.15$ and the blending method.

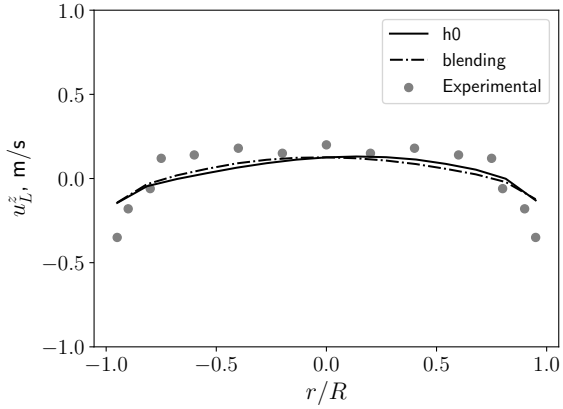

Figure 13: Liquid z-velocity profiles at height $z/D = 3.75$ at $\langle U \rangle = 0.03$ m s^{-1} (homogeneous regime): comparison between the usage of $h_0 = 0.15$ and the blending method.

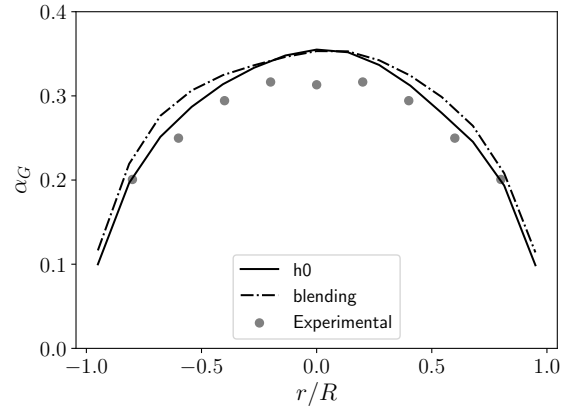

Figure 14: Gas fraction profiles at height $z/D = 2.5$ at $\langle U \rangle = 0.16$ m s^{-1} (heterogeneous regime): comparison between the usage of $h_0 = 0.15$ and the blending method.

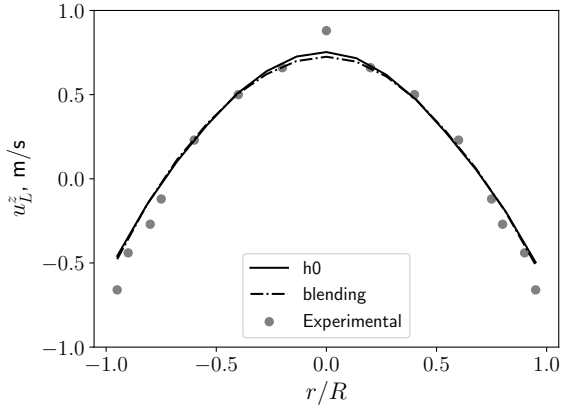

Figure 15: Liquid z-velocity profiles at height $z/D = 3.75$ at $\langle U \rangle = 0.16$ m s^{-1} (heterogeneous regime): comparison between the usage of $h_0 = 0.15$ and the blending method.

not available for multiphase systems: therefore the OpenFOAM results in this work are obtained keeping the standard k-ε.
The outcome of the comparison is shown in Fig. 8 and Fig. 9 for the homogeneous regime and in Fig. 10 and Fig. 11 for the heterogeneous one.
Results indicate that our model provides considerable accuracy in predicting the liquid velocity profiles for both hydrodynamical regimes, especially for the prediction of the liquid axial velocity (Figs. 9,11). In this case, the correspondence between both models and experimental data is maximal. In particular, when the superficial gas velocity is lower (Fig. 9) the values provided by experiments are scattered and do not correspond to the usual quasi-parabolic profiles and a rigorous comparison is harder; nevertheless the standard k-ε model combined with blending produced a flatter profile, closer to the experimental trend.
However, the larger discrepancy was detected in the prediction of the gas fraction profiles (Fig. 8,10) and, in particular, when the superficial gas velocity is equal to 0.16 m s^{-1} (Fig. 10). In this case the trends of the two models differ specularly from the experimental data, reaching the maximum deviation at the center of the column. This behavior is not encountered in the homogeneous regime (Fig. 8) where the profiles are flat and the gap between the two models is non-negligible even closer to the walls.
With the aim to isolate the impact of the turbulence model, a set of simulations was run in `twoPhaseEulerFoam` using the standard k-ε turbulence model and the same swarm factor correction as in (Gemello *et al.*, 2018) with $h_0 = 0.15$. What stands out from results (Figs. 12–15) is that the turbulence modeling has a remarkably stronger impact than the usage of the blending method on the final results. The gap displayed by the two models is now considerably reduced, especially for the prediction of the liquid velocity field: this indicates that the gap reported in Fig. 10 was evidently due to the different k-ε turbulence models used, combined with the high gas velocity.
It may be thus suggested that the implementation of the blending method, if performed with a proper choice of parameters as discussed above, does not affect the fluid dynamical description of two-phase systems.

Computational effort

The capability of the blending method to determine cell by cell the dispersed and the continuous phase and to use the corresponding interphase law allows a significant gain in computational speed. Fig. 16 reports the simulation elapsed time at different gas superficial velocities using 4 processing units Intel Xeon E5-2680 v3 2.50 GHz.
In every case the implementation of blending halved the computational time, without any accuracy loss in results. As pointed out above, this impressive speed up may be linked to description of the head space of the column according to the blending method: if not used, the solver still treats any amount of water in it as continuous phase. This generates huge numerical issues in the computation of the drag force, because it is designed for a dispersion of air in water, and consequently of velocity, k and ε. Contrarily, the activation of the blending allows the recognition of the phase inversion and the water is treated as dispersed phase, using the adequate interphase forces correlations.

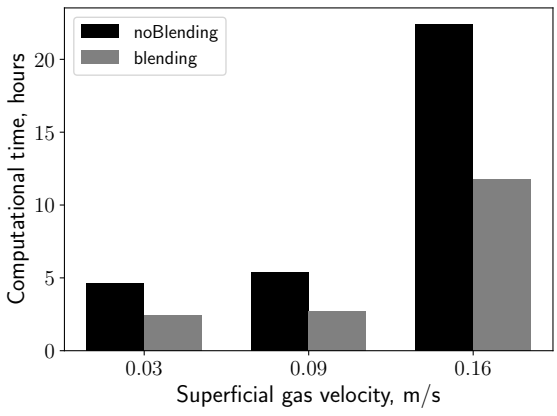

Figure 16: Computational time required by simulations with and without blending implementation.

CONCLUSION

Air-water bubble columns were simulated with OpenFOAM 5.0 using the blending factor approach to model properly interphase forces. After having performed a sensitivity study on the input parameters, an optimal set of them was proposed for the studied system for the investigated superficial velocities. Comparisons with both other models and experimental data shown that the blending factor method is a valid choice for simulating air-water bubbly flows at high gas hold up. Further studies on different geometries and gas velocities may extend the validity of this choice of parameters, with the possibility to increase or reduce the maximum air fully/partially dispersion fraction values. Nevertheless, the upper limit is the maximum close-packing state of bubbles at which, as aforementioned, the air volume fraction is approximately 0.75 for monodisperse bubbles.
The blending approach provides a more physical modeling of the dynamical dispersion phenomena, preventing the usage of semi-empirical correlations to adjust the numerical issues due to miscalculation in the drag force due to high gas hold-up. This matter is addressed through a definition of a partial dispersion zone, where the drag force impact is soften and eventually vanished when the phase-inversion zone is reached.
An insight of the computational time required by the blending method is then reported, showing how its implementation can significantly drop the CPU wall time by more than 50% at any gas superficial velocity.

ACKNOWLEDGMENTS

Computational resources were provided by HPC@POLITO, a project of Academic Computing within the Department of Control and Computer Engineering at the Politecnico di Torino (`http://www.hpc.polito.it`).

REFERENCES

BASHA, O.M., SEHABIAGUE, L., ABDEL-WAHAB, A. and MORSI, B.I. (2015). "Fischer-Tropsch Synthesis in Slurry Bubble Column Reactors: Experimental Investigations and Modeling - A Review". *International Journal of Chemical Reactor Engineering*, **13(3)**, 201–288.

FLECK, S. and RZEHAK, R. (2019). "Investigation of bubble plume oscillations by Euler-Euler simulation". *Chemical Engineering Science*, **207**, 853–861.

GEMELLO, L., CAPPELLO, V., AUGIER, F., MARCHISIO, D. and PLAIS, C. (2018). "CFD-based scale-up of hydrodynamics and mixing in bubble columns". *Chemical Engineering Research and Design*, **136(69)**, 846–858.

HIBIKI, T. and ISHII, M. (2000). "Two-group interfacial area transport equations at bubbly-to-slug flow transition". *Nuclear Engineering and Design*, **202(1)**, 39 – 76.

ISHII, M. and ZUBER, N. (1979). "Drag coefficient and relative velocity in bubbly, droplet or particulate flows". *AIChE journal*, **25(5)**, 843–855.

KANTARCI, N., BORAK, F. and ULGEN, K.O. (2005). "Bubble column reactors". *Process Biochemistry*, **40(7)**, 2263–2283.

MCCLURE, D.D., KAVANAGH, J.M., FLETCHER, D.F. and BARTON, G.W. (2017). "Experimental investigation into the drag volume fraction correction term for gas-liquid bubbly flows". *Chemical Engineering Science*, **170**, 91–97.

NAUMANN, Z. and SCHILLER, L. (1935). "A drag coefficient correlation". *Z Ver Deutsch Ing*, **77**, 318–323.

OpenCFD (). "OpenFOAM". `https://openfoam.org`. [Online; accessed 20-October-2020].

RAIMUNDO, P.M. (2015). *Analysis and modelization of local hydrodynamics in bubble columns*. Thesis, Université Grenoble Alpes.

RANADE, V.V. (2002). *Computational flow modeling for chemical reactor engineering*. Academic Press.

ROGHAIR, I., LAU, Y.M., DEEN, N.G., SLAGTER, H.M., BALTUSSEN, M.W., Van Sint Annaland, M. and KUIPERS, J.A. (2011). "On the drag force of bubbles in bubble swarms at intermediate and high Reynolds numbers". *Chemical Engineering Science*, **66(14)**, 3204–3211.

SHU, S., VIDAL, D., BERTRAND, F. and CHAOUKI, J. (2019). "Multiscale multiphase phenomena in bubble column reactors: A review". *Renewable Energy*, **141**, 613–631.

SIMONNET, M., GENTRIC, C., OLMOS, E. and MIDOUX, N. (2008). "CFD simulation of the flow field in a bubble column reactor: Importance of the drag force formulation to describe regime transitions". *Chemical Engineering and Processing: Process Intensification*, **47(9-10)**, 1726–1737.

SYED, A.H., BOULET, M., MELCHIORI, T. and LAVOIE, J.M. (2018). "CFD simulation of a slurry bubble column: Effect of population balance kernels". *Computers and Fluids*, **175**, 167–179.

TABIB, M.V., ROY, S.A. and JOSHI, J.B. (2008). "CFD simulation of bubble column-An analysis of interphase forces and turbulence models". *Chemical Engineering Journal*, **139(3)**, 589–614.

TOMIYAMA, A. (1998). "Struggle with computational bubble dynamics". *Multiphase Science and Technology*, **10(4)**, 369–405.

VAN LEER, B. (1974). "Towards the ultimate conservative difference scheme. ii. monotonicity and conservation combined in a second-order scheme". *Journal of Computational Physics*, **14(4)**, 361 – 370.